1.3 μm Laser Array on p-type Substrate Using Selective Oxidation of AlInAs

by *Norihiro Iwai *, Toshikazu Mukaihara *, Nobumitsu Yamanaka *, Mitsumasa Ito *, Satoshi Arakawa *, Hitoshi Shimizu *2 and Akihiko Kasukawa **

ABSTRACT 1.3 μm Al-oxide confined inner stripe (ACIS) lasers and laser arrays on a p-InP substrate using the AlInAs-oxide layer have been demonstrated for low-cost parallel data transmission. First, we investigated the oxidation rate of the $Al_XIn_{1-X}As$ layer grown on InP substrate. The optimum conditions were found to be oxidation temperature = 500°C, layer thickness = 100 nm, and Al-contents = 0.48 (lattice-match) taking oxidation rate and surface morphology into account. The 50nm-thick $Al_{0.48}In_{0.52}As$-oxide layer provides good current blocking for laser applications. Based on the above investigations, an ACIS laser fabricated on a p-InP substrate shows a low threshold current of 4.0 mA and a high slope efficiency of 0.6 W/A. We have also confirmed high reliability for an operating time of over 10,000 hours at 85°C, 5 mW. A 22-channel laser array consisting of an ACIS structure has an average threshold current of 3.98 mA and a standard deviation of 0.42 mA. These results indicate that ACIS lasers or laser arrays are promising candidates for low-cost optical data links.

1. INTRODUCTION

It is preferable to fabricate the laser array on a p-type substrate from the viewpoint of high-frequency operation, because an Si-integrated circuit composed of an npn-type transistor has superior high-speed performance. So far, low threshold buried heterostructure (BH) lasers on a p-InP substrate have been investigated intensively for array application, since low threshold operation is needed to reduce power consumption and system skew, and to simplify the driving circuits [1]. Critical fabrication processes, such as narrow stripe width etching at 1.5 μm and a multiple growth step, are required for BH lasers, which might result in a poor yield for an array containing many devices. Conversely, a ridge waveguide (RWG) laser seems to be very attractive for laser array applications because of its simple structure. Recently, we have demonstrated the high performance of 1.3 μm Al-oxide confined inner stripe (ACIS) lasers using a strain compensated AlAs/InP/AlInAs super-lattice structure [2)-3)]. A current confining layer should be inserted into the p-cladding layer for a low threshold current to prevent current spreading in the cladding layer, since the electrical resistivity of n-type InP is two orders of magnitude lower than that of p-type InP for the same carrier concentration. In this case, the current confinement layer should be located below the active layer. However, achieving an epitaxial growth of highly strained AlAs on InP is very difficult because of the large mismatch of 3.5%, even if a strain compensation technique is applied. Therefore, an AlInAs layer lattice-matched InP substrate is used for selective oxidation [4)-6)].

In this paper we report, for the first time, on the ACIS laser and laser array on a p-InP substrate with an AlInAs-oxide confined structure.

2. OXIDATION OF $Al_XIn_{1-X}As$ LAYER

First, we describe the optimization of the oxidation process and conditions of AlInAs layers. In the case of the $Al_XGa_{1-X}As$ layer on a GaAs substrate, a decrease of the oxidation rate was observed with a decrease of the Al-contents (X) [7)]. The AlInAs layer has a low Al content of 48%. Therefore, we are afraid that the oxidation rate decreases further for the AlInAs layer.

To investigate the dependence of the oxidation rate on layer thickness and Al composition, we have prepared the sample shown in Figure 1. This structure was grown by low-pressure metalorganic chemical vapor deposition (LP-MOCVD) at a growth temperature of 600°C. Trimethylindium (TMIn), triethylgallium (TEGa), and trimethylaluminum (TMAl) were used for group III, and phosphine (PH_3) and arsine (AsH_3) were used for group V.

The sample has three $Al_XIn_{1-X}As$ layers consisting of 50 nm (X = 0.48 and 0.7) and 100 nm (X = 0.48) thick separated by 200nm-thick InP layers. To prepare the samples for selective oxidation, 20 μm-wide ridges were formed by wet chemical etching using SiN_x as an etching mask to

* WA Team, Yokohama R&D Lab.
*2 Semiconductor R&D Center, Yokohama R&D Lab.

expose the $Al_xIn_{1-x}As$ layers at the ridge sidewalls for lateral oxidation. Oxidation was carried out in a horizontal quartz tube in a furnace fed with nitrogen gas passed through a deionized water bubbler maintained at 80°C. The flow rate of nitrogen gas was 3 l/min. We used a furnace with three-zone heater in this study, which enabled us to realize high temperature uniformity within ±1°C. The oxidation temperature (T_a) was varied from 450°C to 520°C. After oxidation, the oxidized width and the surface morphology were observed by scanning electron microscope (SEM) and optical microscope, respectively.

Figure 2 shows the oxidized width versus square root of oxidation time ($t^{1/2}$) as a parameter of the $Al_{0.48}In_{0.52}As$ layer thickness at an oxidation temperature (T_a) of 500°C. The oxidation rate is the best fit for a square root function, which is in agreement with published work on the oxidation of $Al_xIn_{1-x}As$ layer[6]. The oxidation rate of 50nm-thick layer and 100nm-thick layer are 0.19 μm/min$^{1/2}$ and 0.5 μm/min$^{1/2}$, respectively. It is clearly found that an oxidation rate of 100nm-thick layer is faster than that of the 50nm-thick layer, as is reported for selective oxidation of AlAs layer[7].

Figure 3 shows the oxidized width versus square root of oxidation time ($t^{1/2}$) as a function of the Al-contents at an oxidation temperature (T_a) of 500°C. No difference in the oxidation rate of 0.19 μm/min$^{1/2}$ was observed for both Al content of 0.48 (lattice-match) and 0.7 (1.5% tensile-strain). It is found that the oxidation rate are not dependent on Al-contents of 0.48 to 0.7.

A low temperature process would be preferred for device application to prevent deterioration of device characteristics due to unexpected diffusion of a doping material such as Zn. The temperature dependence of oxidation rate on layer thickness (d = 50 nm, 100 nm) is another important factor investigated. The oxidation rate sharply increased with the temperature as shown in Figure 4, however, the surface morphology tended to become hazy due to the desorption of phosphorous at a higher tempera-

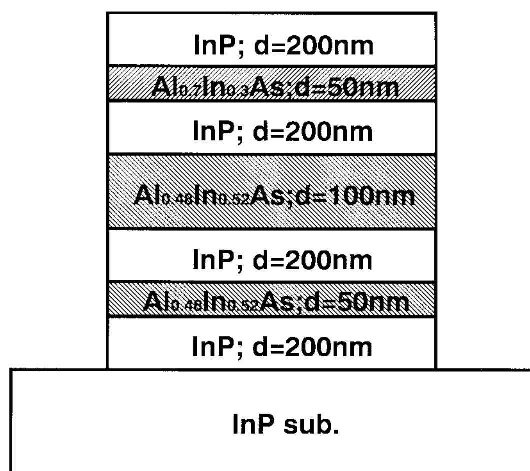

Figure 1 **Schematic diagram of the $Al_xIn_{1-x}As$ layers prepared in this experiment**

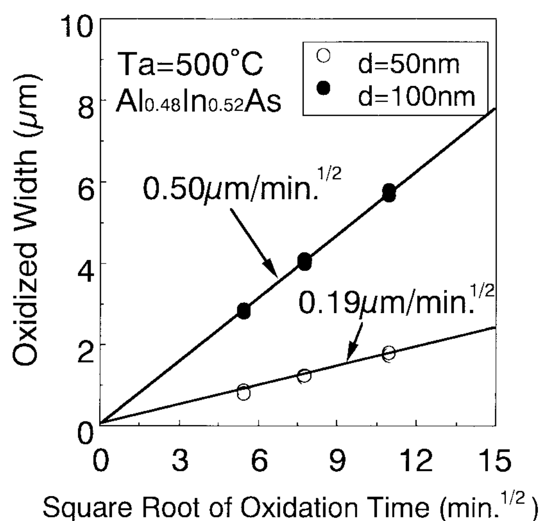

Figure 2 **Oxidized width versus oxidation time as a function of the $Al_{0.48}In_{0.52}As$ layer thickness**

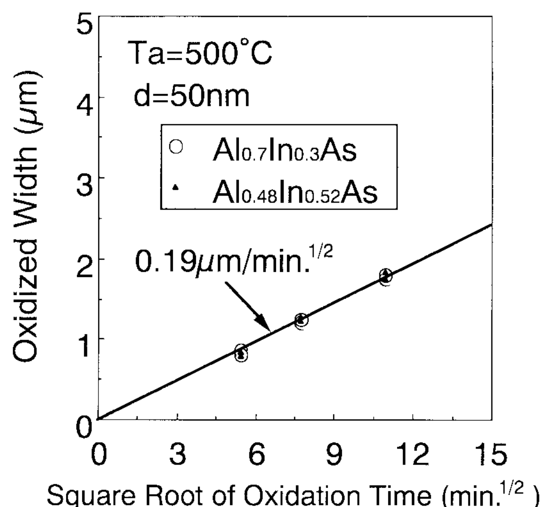

Figure 3 **Oxidized width versus oxidation time as a function of Al content**

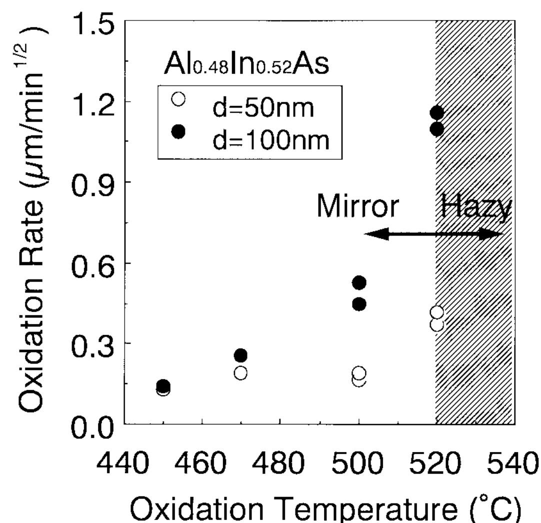

Figure 4 **Temperature dependence of oxidation rate on layer thickness**

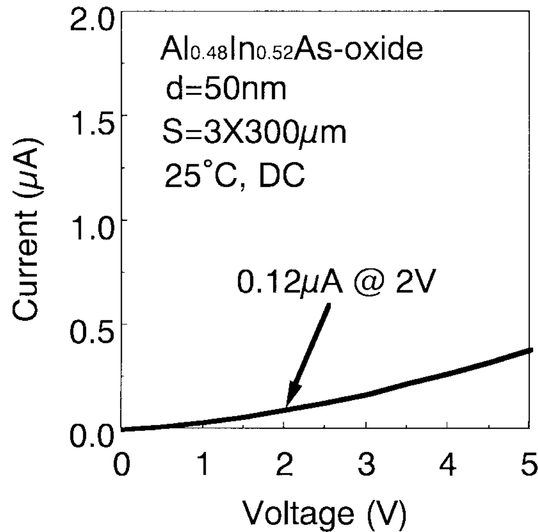

Figure 5 Current-voltage (*I-V*) characteristics of the oxidized $Al_{0.48}In_{0.52}As$ layer

ture (> 520°C).

Current blocking characteristics are very important for laser applications. The room temperature current-voltage (*I-V*) characteristics of the oxidized $Al_{0.48}In_{0.52}As$ layer are shown in Figure 5 for a 3 x 300 μm device with a completely AlInAs-oxide layer. The 50nm-thick $Al_{0.48}In_{0.52}As$ oxidized layer provides good insulation below a bias voltage of 5 V. The leakage current at an applied voltage of 2 V was as low as 0.12 μA, which corresponds to a resistance of 20 MΩ. It was found that the AlInAs-oxide layer provides sufficient current blocking for laser application. All the samples with d = 50 nm and 100 nm oxidized at different oxidation temperatures have similar *I-V* characteristics.

From the above investigations on the oxidation rate, the surface morphology, and the current blocking characteristics, the optimum conditions were found to be oxidation temperature of 500°C, layer thickness of 100 nm, and Al content of 0.48 (lattice-match).

3. ACIS LASERS ON p-TYPE InP SUBSTRATE

As discussed in previous sections, we described the optimum conditions of the oxidation of the AlInAs layer for laser applications. We applied this oxidation technique of AlInAs layer to a ridge waveguide (RWG) laser structure. In this section, we present high-performance Al-oxide confined inner stripe (ACIS) lasers[8].

Figure 6 shows a schematic view of fabricated ACIS laser. Laterally, both optical and current confinements can be realized by the low index, and insulating AlInAs-oxidized layer. The active layer consisted of 1% compressively strained GaInAsP triple-quantum wells (5.5 nm thick each) separated by selectively n-doped (1 x 10^{18} cm^{-3}) GaInAsP barriers with a band gap wavelength of 1.1 μm

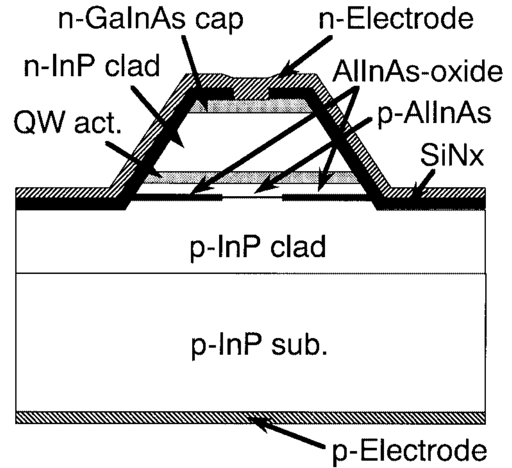

Figure 6 Schematic diagram of the 1.3 μm ACIS laser on p-InP substrate

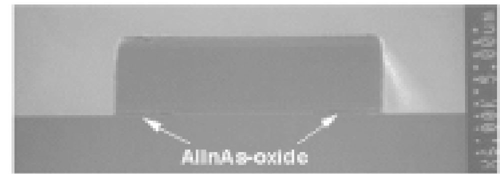

Figure 7 Cross-sectional SEM image after oxidation

(10 nm thick each). Graded-index separate confinement heterostructure (GRIN-SCH) layers, of decreasing bandgap wavelengths of 1.1, 1.05, and 1.0 μm with a layer thickness of 30 nm, are used for the optical confinement layer. The thickness of the AlInAs layer is 100 nm. The distance between the active layer and the oxidized layers is set at 200 nm, which is decided by considering induced stress and other factors. All the layers are grown by LP-MOCVD on a p-InP substrate at a growth temperature of 600°C.

The ridge stripe width of 10 μm, for exposing the edge of the AlInAs layer for oxidation, is formed by reactive ion beam etching (RIBE) using SiN_x as an etching mask. Oxidation is performed at 500°C in nitrogen gas that is bubbled through water at 80°C. Figure 7 shows the cross-sectional SEM view of the oxidized AlInAs layers. The oxide opening (= current aperture) defined is about 5.0 μm after 90 min of oxidation.

After oxidation, the sample is processed into a conventional ridge waveguide structure. It should be noted that the fabrication process is quite easy, since the initial ridge width is as wide as 10 μm.

The pulsed and CW light output power versus injection current (*L/I*) characteristics are shown in Figure 8 for a 400 μm long ACIS laser at 25°C. The ACIS laser was coated with a high reflective (HR) coating on a back facet (R_f/R_b = 30% / 96%). A low threshold current of 12.9 mA and a high slope efficiency of 0.6 W/A were obtained. Moreover, light output power of 100 and 90 mW were obtained at pulsed and CW operations, respectively.

We designed the cavity structure so that a low threshold

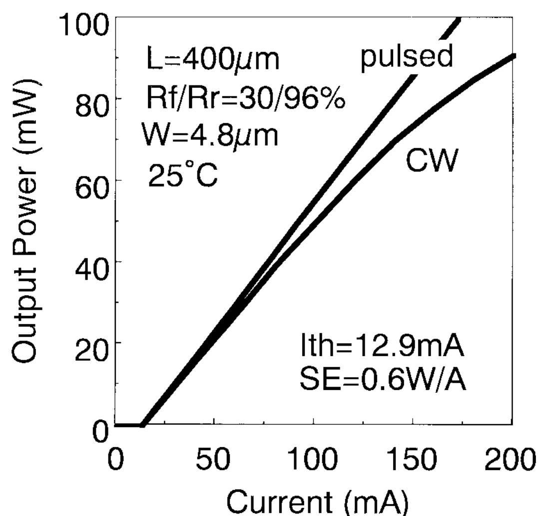

Figure 8 ***L/I*** **characteristics of an ACIS laser**

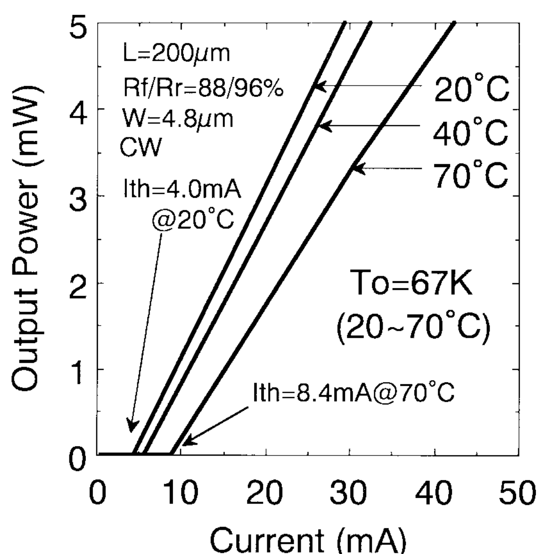

Figure 9 **Temperature dependence of** ***L/I*** **characteristics of an ACIS laser**

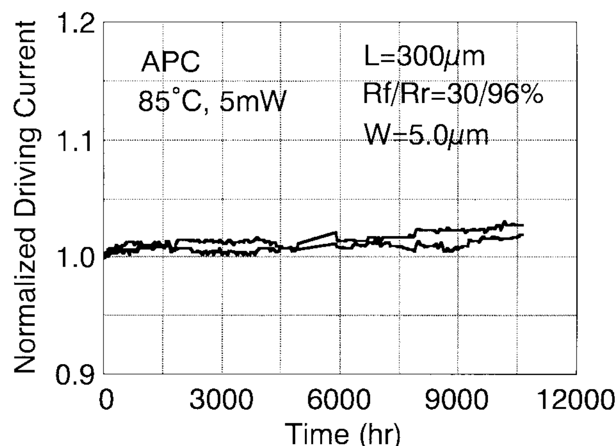

Figure 10 **Aging characteristics of the ACIS lasers**

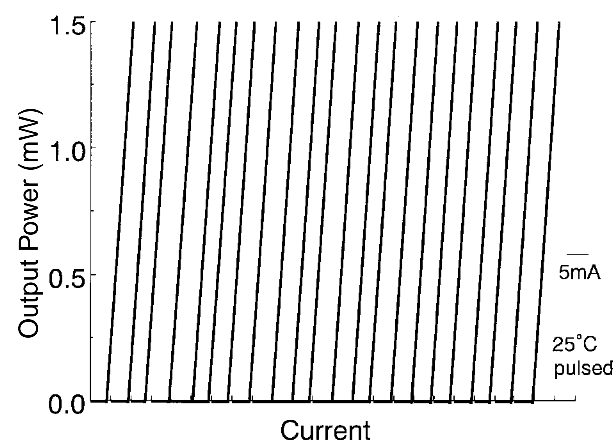

Figure 11 **Pulsed** ***L/I*** **characteristics of the consecutive 22-channel ACIS laser array**

current can be obtained with the combination of a short cavity of 200 μm and HR coatings on both facets (R_f/R_b = 88% / 96%). The temperature dependence of the *L/I* characteristics is shown in Figure 9. A low threshold current of 4.0 mA at 20°C, which corresponds to a threshold current density as low as 420 A/cm^2, was obtained. A lower threshold current can be expected for a device with a narrower current aperture. The characteristic temperature was measured to be 67 K in the temperature range 20 to 70°C.

Both low threshold current and high power operation indicate that the Al-oxide layer using the AlInAs layer provides good current confinement.

The aging test at 85°C, 5 mW are shown in Figure 10 for the Cleave / HR ACIS lasers in the automatic power control (APC) mode. No appreciable change in driving currents was observed after 10,000 hours. The increasing rate of driving current was about 1%/khr, and it tends to saturate. We can expect more than 10^6 hours by extrapolating this curve if the end of life is defined as a 20% increase of the driving current.

4. ACIS LASER ARRAY

The pulsed *L/I* characteristics of the consecutive 22-channel laser array[9] are shown in Figure 11. The average of the threshold currents was 3.98 mA and the standard deviation was 0.42 mA. This standard deviation is 10% of the threshold current, which is comparable to conventional BH lasers. This preliminary result indicates that an ACIS laser is one of the promising candidates for a laser array on a p-InP substrate due to its simple structure.

5. CONCLUSION

In conclusion, we investigated the selective oxidation of $Al_xIn_{1-x}As$ layers grown on p-InP for the laser array applications. It is experimentally found that the oxidation rate increases with the layer thickness and the oxidation tem-

perature, and there is no difference in the Al contents in the range of 0.48 to 0.7. The measured electrical property of 50nm-thick $Al_{0.48}In_{0.52}As$-oxide layer shows a good current blocking characteristic.

Based on the above results, we have fabricated a high-performance 1.3 µm ACIS laser and laser array, together with promising aging characteristics for the first time. The high-performance lasing characteristics obtained in this study show the possibility of a low-cost, high-performance, long-wavelength laser for low-cost optical data links.

ACKNOWLEDGMENTS

The authors are grateful to Dr. Y. Suzuki and J. Kikawa for their constant encouragement, Dr. N. Yokouchi, M. Funabashi, K. Hiraiwa and H. Shimizu for valuable discussions, F. Iwase, T. Matsuda, Y. Murayama and K. Yabusaki for SEM observations.

REFERENCES

1) K. Uomi, T. Tsuchiya, M. Komori, A. Oka, T. Kawano, and A. Oishi: IEEE J. Select. Topics Quantum Electron., 1, (1995), 203.
2) N. Iwai, T. Mukaihara, H. Shimizu, N. Yamanaka, K. Kumada, and A. Kasukawa: Electron. Lett., 34, (1998), 890.
3) N. Iwai, T. Mukaihara, N. Yamanaka, K. Kumada, H. Shimizu, and A. Kasukawa: IEEE J. Select. Topics Quantum Electron., 5, (1999), 694.
4) S. J. Caracci, M. R. Krames, N. Holonyak: J. Appl. Phys., 75, (1994), 2706.
5) H. Takenouchi, T. Kagawa, Y. Ohiso, T. Tadokoro, and T. Kurokawa: Electoron. Lett., 32, (1995), 1671.
6) H. Gebretsadik, K. Kamath, W-D. Zhou, and P. Bhattacharya: Appl. Phys. Lett., 72, (1998), 135.
7) K. D. Choquette, K. M. Geib, C. I. H. Ashby, R. D. Twesten, O. Blum, Q. Hou, D. M. Follstaedt, B. E. Hammons, D. Mathes, and R. Hull: IEEE J. Select. Topics Quantum Electron., 3, (1997), 916.
8) N. Iwai, T. Mukaihara, N. Yamanaka, M. Ito, S. Arakawa, H. Shimizu, and A. Kasukawa: Electron. Lett., 34, (1998), 1427.
9) N. Iwai, T. Mukaihara, N. Yamanaka, M. Ito, S. Arakawa, H. Shimizu, and A. Kasukawa: Electron. Lett., 35, (1999), 1081.

Manuscript received on December 18, 2000.